FINITE ELEMENT DEVELOPMENT FOR GENERALLY SHAPED PIEZOELECTRIC ACTIVE LAMINATES PART II – GEOMETRICALLY NONLINEAR APPROACH

UDC 515.3 : 624.041/046

Dragan Marinković[1,2], Heinz Köppe[1], Ulrich Gabbert[1]

[1]Otto-von-Guericke-Universität Magdeburg, Fakultät für Maschinenbau,
Institut für Mechanik, Universitätsplatz 2, D-39106 Magdeburg, Germany
[2]Faculty of Mechanical Engineering, University of Niš
Aleksandra Medvedeva 14, 18000 Niš, Serbia and Montenegro

Abstract. *Piezoelectric thin-walled structures, especially those with a notably higher membrane than bending stiffness, are susceptible to large transverse deflections. In the recent years numerical investigations conducted by different researchers have shown that the deflection amplitude, vibration frequency, output voltage and other values of interest can be significantly influenced by the assumption of large displacements and deformations of the structure. Therefore, the second part of the paper extends the formulation given in the first part into the geometrically nonlinear analysis, adopting the assumption of small strains but large displacements. The co-rotational approach is used. The linearized finite element equations for the geometrically nonlinear analysis of the piezoelectric continuum are developed and applied by means of the 9-node degenerated shell element described in the first part of the paper.*

Key Words: *Geometrically Nonlinear Analysis, Active Structure, Finite Shell Element, Piezoelectric Components*

1. INTRODUCTION

The potential benefits of active structures in various applications have attracted numerous researchers to devote their work to this area, especially in the field of modeling. The main objectives of the modeling are often quite opposite – on the one hand, a model is supposed to offer a satisfying accuracy, but on the other hand, the required numerical effort should not be too great. Hence, a compromise is to be made. As a rule, the linear analysis is numerically less demanding than the nonlinear analysis. However, in the recent years numerical results from different researchers have shown that the deflection amplitude, vibration frequency, output voltage and other values of interest can be significantly

influenced by the assumption of large displacements and deformations of the structure. Therefore, a number of different finite element formulations pertaining to the thin-walled active structures, which take into account geometrically and/or materially nonlinear effects, have been developed. A few of them will be mentioned here.

Yi et al. [12] have developed a 20-node solid element for the nonlinear analysis of the laminated adaptive structures using the updated Lagrangian formulation. Simoes Moita et al. [10] have developed a 3-node triangular piezolaminated facet element based on the classical theory, i.e. the Kirchhoff kinematical assumption is considered, for the static geometrically nonlinear analysis. Utilizing a laminate theory of higher order, Carrera [5] has developed a plate element, with the zig-zag effect included and the interlaminar equilibrium was fulfilled for resolving the transverse shear stresses. The geometrically nonlinear analysis with the von-Kármán type nonlinearities and a quadratic distribution of the electric potential along the thickness were considered. Varelis and Saravanos [11] have described a mixed finite element formulation to capture nonlinear effects in the bucking analysis of adaptive piezoelectric composite plates. Mesecke-Rischmann [8] has developed a mixed formulation of the shallow shell and the nonlinear material constitutive equations were included. It should be emphasized that it was not the authors' intention hereby to give an exhaustive survey of the nonlinear finite element formulations for adaptive structures, but only to represent the general basis of the development.

Generally shaped structures made of piezoelectric composite laminates are arbitrarily curved thin-walled structures. Due to the considerably smaller thickness with respect to the in-plane dimensions these structures are susceptible to relatively large transverse deflections, still exhibiting small strains. This case qualifies for the geometrically nonlinear analysis and it will be a subject of our consideration in the sequel.

2. GEOMETRICALLY NONLINEAR ANALYSIS IN THE FINITE ELEMENT FORMULATION

Let's consider a motion of a piezoelectric active structure in the global Cartesian system assuming that the structure undergoes large displacements, but small strains. The Lagrangian (material) formulation of the problem seems to be a natural and convenient choice, since we follow all particles of the structure in their motion.

An incremental step-by-step approach represents a usual solution strategy in the nonlinear analysis. It assumes that the solution for the discrete time t is known, and seeks the solution at the discrete time $t + \Delta t$, with a suitably chosen time increment Δt. The solution at each discrete time t, i.e. the structure configuration, has to be determined so as to satisfy the equilibrium condition:

$$^{t}\{F\} = {}^{t}\{R\} \, , \tag{1}$$

where $^{t}\{R\}$ comprises all external (body, surface and point) generalized forces (mechanical forces and electrical charges), as well as inertia and damping forces in the case of the dynamic analysis, and $^{t}\{F\}$ are the generalized internal forces, the mechanical part of which is given as:

$$^{t}\{f_{int}\} = \int_{^{t}V} {}^{t}[B_{L}]^{T} {}^{t}\{\sigma\} \, d^{t}V \ , \tag{2}$$

where $^{t}[B_{L}]$ is the linear strain-displacement matrix described in [6], $^{t}\{\sigma\}$ is the engineering (Cauchy) stress vector (Voigt notation used), and ^{t}V the structure domain, all of them with respect to the configuration at time t.

It can be noticed that time is included in the calculation, regardless of the type of analysis, i.e. whether we deal with static or dynamic analysis. In the static analysis it is only a convenient auxiliary variable used to denote gradually increasing loads, and in the dynamic analysis it is an actual variable, since loads are defined as time functions.

Since the geometrically nonlinear analysis recognizes that the structure takes different configurations during the loading, all the quantities of interest have to be defined with respect to certain configuration. It could be any of the determined configurations, starting from the initial one. It is quite logical to choose either the initial configuration or the last calculated configuration, i.e. at time t. The former choice is characteristic for the total Lagrangian formulation, and the latter is used within the updated Lagrangian configuration. Both formulations yield the same result when used in their pure form, i.e. without any approximations. The choice between them depends on the material constitutive law and the numerical effectiveness. The updated formulation allows higher numerical effectiveness when certain assumptions are included. There is another important advantage considering the updated formulation. It facilitates the introduction of anisotropic nonlinear material properties in the analysis and allows in that manner the extension of the formulation into the "full" (geometrically and materially) nonlinear analysis. Therefore, our attention will be focused on the updated Lagrangian formulation.

3. STRAIN AND STRESS MEASURES IN UPDATED FORMULATION

Observe the structure in Fig. 1. Assume that it is in a pre-stressed state and that it performs a rigid-body motion from configuration 1 to configuration 2. Obviously, the strain and the stress state of the structure are not affected by the performed rigid-body motion. However, the tensors describing them with respect to the fixed global coordinate system (x, y, z), with respect to which the motion of the structure is described as well, have changed. This simple case represents the essence of the problem that the geometrically nonlinear analysis has to deal with. Two different approaches are possible in order to solve the problem. The first approach consists in the introduction of auxiliary strain and stress measures with special characteristics as will be seen in the sequel of the section. The second, co-rotational approach implies the introduction of an auxiliary (co-rotational) coordinate system fixed to the structure (such as (x′, y′, z′) in Fig. 1). The basic features of both approaches will be briefly described in the sequel.

The actual (engineering) strain and stress measures in certain configuration are referred to the very same configuration. In order to calculate a new configuration it is needed to determine the actual stress field in it (see relations (1) and (2)), and within the frame of the nonlinear analysis the new configuration is still unknown. One of the possible ways to deal with the problem of continuously changing configuration is the
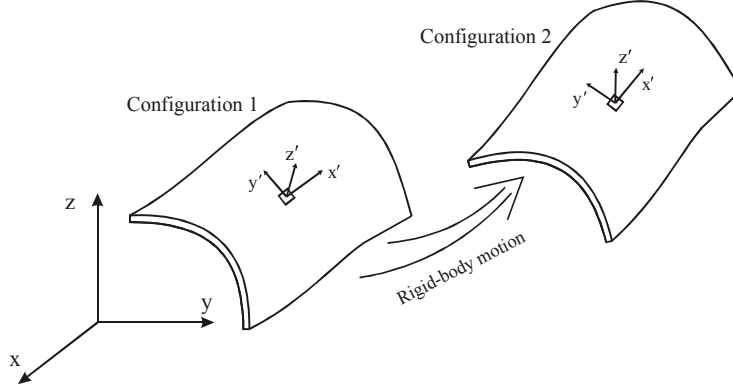
Fig. 1. Rigid-body motion of a structure from configuration 1 to configuration 2

introduction of auxiliary strain and stress measures. The aim of their introduction is to express the internal virtual work performing the integration over the domain of a known structure configuration, and to be able to incrementally decompose the strains and the stresses in an effective manner. Various strain and stress measures can be used, but only the most frequently used will be briefly mentioned here, and those are the Green-Lagrange strain and the 2nd Piola-Kirchhoff stress, work conjugate with each other (the integral of their product over the domain of the reference configuration gives the internal virtual work).

In the coordinate system (x_1, x_2, x_3) with displacements (u_1, u_2, u_3) the Green-Lagrange strain field is given in the following general form:

$$\varepsilon_{ij}^{GL} = \frac{1}{2}\left(\frac{\partial u_i}{\partial x_j} + \frac{\partial u_j}{\partial x_i} + \frac{\partial u_k}{\partial x_i}\frac{\partial u_k}{\partial x_j}\right), \tag{3}$$

where the summation on the repeated index k is applied.

Since the updated formulation is considered, the quantities of interest shall be given at time $t + \Delta t$, at which the structure configuration is sought (denoted by left superscript), but with respect to the last calculated configuration, i.e. the configuration at time t (denoted by left subscript[1]). If this is not so, it will be outlined. Taking this remark into account, the Green-Lagrange strain measure can be rewritten in the condensed form:

$$_t^{t+\Delta t}\{\varepsilon_{GL}\} = {_t^{t+\Delta t}}\{\varepsilon\} + {_t^{t+\Delta t}}\{\eta\}, \tag{4}$$

where ${_t^{t+\Delta t}}\{\varepsilon\}$ is the linear term, and ${_t^{t+\Delta t}}\{\eta\}$ is the nonlinear term. Now, the Green-Lagrange strain tensor can be interpreted as being equal to the engineering strain tensor in a system rigid-body rotating with the particle [7]. Therefore, a relation between the engineering strain tensor and the Green-Lagrange strain tensor at time $t + \Delta t$ can be established by means of deformation gradient matrix:

---

[1] The system of notation follows Bathe [1]

$$^{t+\Delta t}_{\quad t}[\varepsilon_{GL}] = {}^{t+\Delta t}_{\quad t}[F]^T \, {}^{t+\Delta t}[\varepsilon] \, {}^{t+\Delta t}_{\quad t}[F] \quad \text{or} \quad {}^{t+\Delta t}[\varepsilon] = {}^{t+\Delta t}_{\quad t}[F]^{-T} \, {}^{t+\Delta t}_{\quad t}[\varepsilon_{GL}] \, {}^{t+\Delta t}_{\quad t}[F]^{-1} , \tag{5}$$

where $^{t+\Delta t}_{\quad t}[F]$ represents the deformation gradient matrix:

$$^{t+\Delta t}_{\quad t}[F] = \begin{bmatrix} \dfrac{\partial\,^{t+\Delta t}x_1}{\partial\,^t x_1} & \dfrac{\partial\,^{t+\Delta t}x_1}{\partial\,^t x_2} & \dfrac{\partial\,^{t+\Delta t}x_1}{\partial\,^t x_3} \\[2mm] \dfrac{\partial\,^{t+\Delta t}x_2}{\partial\,^t x_1} & \dfrac{\partial\,^{t+\Delta t}x_2}{\partial\,^t x_2} & \dfrac{\partial\,^{t+\Delta t}x_2}{\partial\,^t x_3} \\[2mm] \dfrac{\partial\,^{t+\Delta t}x_3}{\partial\,^t x_1} & \dfrac{\partial\,^{t+\Delta t}x_3}{\partial\,^t x_2} & \dfrac{\partial\,^{t+\Delta t}x_3}{\partial\,^t x_3} \end{bmatrix} = \begin{bmatrix} 1+\dfrac{\partial\,^t\Delta u_1}{\partial\,^t x_1} & \dfrac{\partial\,^t\Delta u_1}{\partial\,^t x_2} & \dfrac{\partial\,^t\Delta u_1}{\partial\,^t x_3} \\[2mm] \dfrac{\partial\,^t\Delta u_2}{\partial\,^t x_1} & 1+\dfrac{\partial\,^t\Delta u_2}{\partial\,^t x_2} & \dfrac{\partial\,^t\Delta u_2}{\partial\,^t x_3} \\[2mm] \dfrac{\partial\,^t\Delta u_3}{\partial\,^t x_1} & \dfrac{\partial\,^t\Delta u_3}{\partial\,^t x_2} & 1+\dfrac{\partial\,^t\Delta u_3}{\partial\,^t x_3} \end{bmatrix}, \tag{6}$$

with Δ denoting the increment of the quantity of interest between two successive configurations.

Similarly, the 2nd Piola-Kirchhoff stress tensor, $^{t+\Delta t}_{\quad t}[S]$, can be related to the Cauchy (engineering) stress tensor at time t+Δt, $^{t+\Delta t}[\sigma]$, via:

$$^{t+\Delta t}_{\quad t}[S] = \det[F] \, {}^{t+\Delta t}_{\quad t}[F]^{-1} \, {}^{t+\Delta t}[\sigma] \, {}^{t+\Delta t}_{\quad t}[F]^{-T} \quad \text{or} \quad {}^{t+\Delta t}[\sigma] = \frac{1}{\det[F]} \, {}^{t+\Delta t}_{\quad t}[F] \, {}^{t+\Delta t}_{\quad t}[S] \, {}^{t+\Delta t}_{\quad t}[F]^T \tag{7}$$

A similar interpretation as for the Green-Lagrange strain can be made here [7]: the 2nd Piola-Kirchhoff stress tensor is equal to the Cauchy stress tensor in a system rigid-body rotating with a particle.

The 2nd Piola-Kirchhoff stress vector can also be related to the Green-Lagrange strain vector, through the material constitutive law:

$$^{t+\Delta t}_{\quad t}\{S\} = {}^{t+\Delta t}_{\quad t}[C] \, {}^{t+\Delta t}_{\quad t}\{\varepsilon_{GL}\} . \tag{8}$$

The Green-Lagrange strain and the 2nd Piola-Kirchhoff stress exhibit very important properties. They do not change when a structure undergoes a rigid-body motion [1]. As a consequence, they can be incrementally decomposed, so that it can be written:

$$^{t+\Delta t}_{\quad t}\{S\} = {}^t\{\sigma\} + {}_t\{S\} , \tag{9}$$

where $^t\{\sigma\}$ is the Cauchy (actual) stress, and $_t\{S\}$ is the incremental 2nd Piola-Kirchhoff stress due to incremental displacements, both at time t, and it should be noted that $^t_t\{S\} \equiv {}^t\{\sigma\}$. A similar equation is valid for the incremental decomposition of the strain.

The second approach to the problem is the so-called co-rotational approach. As it was pointed out by the example in Fig. 1, although the rigid-body motion does not affect the strain and stress state of the structure, their tensor representation with respect to the fixed coordinate system do change. However, the tensor representation with respect to the co-ordinate system fixed to the structure would not change. Hence, the term "co-rotational" is taken here to relate to the provision of an auxiliary coordinate system that continuously rotates with the structure and with respect to which small strain-small displacement (or engineering [4]) relationship can be applied, provided small incremental steps are used. Belytschko et al. [2, 3] applied the co-rotational approach to dynamic analysis using an

explicit formulation, which itself requires small time-steps due to the stability require-
ments of the method. Generally speaking, a structure fixed coordinate system can be pro-
vided at each point of the discretized representation of the structure. Furthermore, such a
coordinate system, namely the structure reference system, was already introduced in the
first part of the paper for the purpose of modeling generally shaped composite laminates.
The introduction of this coordinate system was necessary primarily due to the non-iso-
tropic material properties. It requires the calculation of the strain and stress field with
respect to the very same reference frame. Thus, this coordinate system can also be taken
advantage of in order to extend the linear formulation into the geometrically nonlinear
one and this approach is used in the present work.

4. FINITE ELEMENT EQUATIONS

The piezoelectric continuum equation for the geometrically nonlinear analysis using
the updated Lagrangian relates two successive system configurations (let's say at time
$t + \Delta t$ and t), whereby all the quantities are referred to the last determined system configu-
ration. The choice between the static and the dynamic analysis, i.e. whether to include
inertia and damping forces or not, is a matter of the engineering judgment (just as for the
linear or the nonlinear analysis). The static analysis demands less numerical effort, but
one should be cautious on that matter – the choice of the static analysis needs to be justi-
fied, otherwise the predicted behavior of the structure might suffer on accuracy. The
scope of this paper covers only the static analysis.

In the nonlinear static analysis time is included only to denote gradually increasing
loads. The whole load set is partitioned into a number of increments. After determining
the structure configuration at time t, a new load increment is imposed, and a new structure
configuration is sought so as to satisfy the equilibrium condition with the dynamic effects
neglected. The Hamilton's principle for the piezoelectric continuum applied between two
successive structure configurations yields:

$$\delta \, ^t\Delta H = \delta(^{t+\Delta t}\Delta W_{ext} - \, ^t\Delta W_{int}) \tag{10}$$

which represents the energy balance throughout the incremental displacements:

Incremental electric enthalpy =
Work of external forces at time ($t + \Delta t$) throughout incremental displacements $\{\Delta u\}$ –
Work of internal forces at time (t) throughout incremental displacements $\{\Delta u\}$

The developed form of equation (10) is given as:

$$\int_{^tV} [\{\delta \Delta \varepsilon\}^T [C^E]\{\Delta \varepsilon\} - \{\delta \Delta \varepsilon\}^T [e]^T \{\Delta E\} - \{\delta \Delta E\}^T [e]\{\Delta \varepsilon\} - \{\delta \Delta E\}^T [d^\varepsilon]\{\Delta E\}] dV =$$

$$= \{\delta \Delta u\}^T \{^{t+\Delta t} F_{ext}\} - \int_{^tV} \{\delta \Delta \varepsilon\}^T \, ^t\{\sigma\} dV - \delta \Delta \phi \, ^{t+\Delta t}Q_{ext} + \int_{^tV} \{\delta \Delta E\}^T \, ^t\{D\} dV \; , \tag{11}$$

Performing the discretization of the structure and using the element incremental nodal displacements and potentials vectors, equation (11) results in the following linearized system of equations on the element level:

$$\int_{{}^t V} {}^t[B_L]^T[C^E]\,{}^t[B_L]\mathrm{d}\,{}^t V\,{}^t\{\Delta u_e\} + \int_{{}^t V} {}^t[G]^T\,{}^t[\sigma]\,{}^t[G]\mathrm{d}V\,{}^t\{\Delta u_e\} + \int_{{}^t V} {}^t[B_L]^T[e]\,{}^t[B_\phi]\mathrm{d}V\,{}^t\{\Delta\phi_e\} =$$

$$= \int_{{}^t V} [N_u]^T\,{}^{t+\Delta t}\{F_V\}\,\mathrm{d}V + \int_{{}^t S_1} [N_u]^T\,{}^{t+\Delta t}\{F_{S_1}\}\,\mathrm{d}S_1 + [N_u]^T\,{}^{t+\Delta t}\{F_{Pe}\} - \int_{{}^t V} {}^t[B_L]^T\,{}^t\{\sigma\}\mathrm{d}V, \qquad (12)$$

$$\int_{{}^t V} {}^t[B_\phi]^T[e]^T\,{}^t[B_L]\mathrm{d}V\,{}^t\{\Delta u_e\} - \int_{{}^t V} {}^t[B_\phi]^T[d^\varepsilon]\,{}^t[B_\phi]\mathrm{d}V\,{}^t\{\Delta\phi_e\} =$$

$$= -\int_{{}^t S_2} {}^t[N_\phi]^T\,{}^{t+\Delta t}\{q\}\,\mathrm{d}S_2 - {}^t[N_\phi]^T\,{}^{t+\Delta t}\{Q_e\} - \int_{{}^t V} {}^t[B_\phi]^T\,{}^t\{D\}\mathrm{d}V, \qquad (13)$$

where ${}^t[G]$ represents the displacements derivatives matrix. In coordinate system (x, y, z) with displacements (u, v, w) it will be:

$$[G]\{u\} = \left\{ \frac{\partial u}{\partial x} \quad \frac{\partial u}{\partial y} \quad \frac{\partial u}{\partial z} \quad \frac{\partial v}{\partial x} \quad \frac{\partial v}{\partial y} \quad \frac{\partial v}{\partial z} \quad \frac{\partial w}{\partial x} \quad \frac{\partial w}{\partial y} \quad \frac{\partial w}{\partial z} \right\}^T \qquad (14)$$

The reason for the presence of matrix [G] in equation (12) becomes more obvious after noting that the nonlinear part of the strain field (see (3)) can be represented in the following way:

$$\{\eta\} = \begin{bmatrix} \frac{\partial u}{\partial x} & 0 & 0 & \frac{\partial v}{\partial x} & 0 & 0 & \frac{\partial w}{\partial x} & 0 & 0 \\ 0 & \frac{\partial u}{\partial y} & 0 & 0 & \frac{\partial v}{\partial y} & 0 & 0 & \frac{\partial w}{\partial y} & 0 \\ 0 & 0 & \frac{\partial u}{\partial z} & 0 & 0 & \frac{\partial v}{\partial z} & 0 & 0 & \frac{\partial w}{\partial z} \\ \frac{\partial u}{\partial y} & \frac{\partial u}{\partial x} & 0 & \frac{\partial v}{\partial y} & \frac{\partial v}{\partial x} & 0 & \frac{\partial w}{\partial y} & \frac{\partial w}{\partial x} & 0 \\ \frac{\partial u}{\partial z} & 0 & \frac{\partial u}{\partial x} & \frac{\partial v}{\partial z} & 0 & \frac{\partial v}{\partial x} & \frac{\partial w}{\partial z} & 0 & \frac{\partial w}{\partial x} \\ 0 & \frac{\partial u}{\partial z} & \frac{\partial u}{\partial y} & 0 & \frac{\partial v}{\partial z} & \frac{\partial v}{\partial y} & 0 & \frac{\partial w}{\partial z} & \frac{\partial w}{\partial y} \end{bmatrix} [G]\{u\} = [A(\{u\})][G]\{u\} \quad (15)$$

where $[A(\{u\})]$ is the part of the nonlinear strain-displacement matrix that is used in the total Lagrangian formulation since all the quantities are referred to the initial configuration and it depends on the initial displacements [4]. In the updated Lagrangian configura-

tion there is no initial displacement effect because the last determined configuration is "frozen" and all the quantities are referred to it.

Matrix ${}^{t}[B_L]$ in (12) is the strain-displacement matrix used in the linear analysis, and $[\sigma]$ is the engineering stress matrix in the last determined system configuration of the following general form:

$$[\overline{\sigma}] = \begin{bmatrix} \sigma_{xx} & \sigma_{xy} & \sigma_{xz} \\ \sigma_{xy} & \sigma_{yy} & \sigma_{yz} \\ \sigma_{xz} & \sigma_{yz} & \sigma_{zz} \end{bmatrix} \Rightarrow [\sigma] = \begin{bmatrix} [\overline{\sigma}] & [0] & [0] \\ [0] & [\overline{\sigma}] & [0] \\ [0] & [0] & [\overline{\sigma}] \end{bmatrix}, \tag{16}$$

and, ${}^{t}\{\Delta u_e\}$ and ${}^{t}\{\Delta\phi_e\}$ are the incremental element nodal displacements and potentials vectors, respectively. All quantities are defined at time t, which corresponds to the last calculated configuration.

Using the notation characteristic for the finite element method the following abbreviated form of (12) and (13) is obtained:

$${}^{t}[K_{uuT}] \, {}^{t}\{\Delta u_e\} + {}^{t}[K_{u\phi}] \, {}^{t}\{\Delta\phi_e\} = {}^{t+\Delta t}\{f_{ext_e}\} - {}^{t}\{f_{int_e}\} \tag{17}$$

$${}^{t}[K_{\phi u}] \, {}^{t}\{\Delta u_e\} + {}^{t}[K_{\phi\phi}] \, {}^{t}\{\Delta\phi_e\} = {}^{t+\Delta t}\{q_{ext_e}\} - {}^{t}\{q_{int_e}\} \tag{18}$$

where ${}^{t}[K_{uuT}]$ represents the mechanical tangential stiffness matrix:

$${}^{t}[K_{uuT}] = \int_{{}^{t}V} {}^{t}[B_L]^T [C^E] \, {}^{t}[B_L] d \, {}^{t}V + \int_{{}^{t}V} {}^{t}[G]^T \, {}^{t}[\sigma] \, {}^{t}[G] d \, {}^{t}V \tag{19}$$

the piezoelectric coupling and dielectric stiffness matrix are given as:

$${}^{t}[K_{u\phi}] = \int_{{}^{t}V} {}^{t}[B_L]^T [e] \, {}^{t}[B_\phi] dV = {}^{t}[K_{\phi u}]^T \tag{20}$$

$${}^{t}[K_{\phi\phi}] = -\int_{{}^{t}V} {}^{t}[B_\phi]^T [d^\varepsilon] \, {}^{t}[B_\phi] dV \tag{21}$$

and, finally, ${}^{t}\{f_{inte}\}$ and ${}^{t}\{q_{inte}\}$ are the element internal forces and electric charges vectors, respectively, defined as:

$${}^{t}\{f_{int_e}\} = \int_{{}^{t}V} {}^{t}[B_L]^T \, {}^{t}\{\sigma\} dV, \tag{22}$$

$${}^{t}\{q_{int_e}\} = \int_{{}^{t}V} {}^{t}[B_\phi]^T \, {}^{t}\{D\} dV, \tag{23}$$

and ${}^{t+\Delta t}\{f_{exte}\}$ and ${}^{t+\Delta t}\{q_{exte}\}$ comprise the element external forces and electric charges.

Introducing generalized element tangential stiffness matrix $[K_T]$, generalized incremental element displacements vector $\{\Delta U_e\}$, generalized element external forces $\{R_e\}$ and generalized element internal forces $\{F_e\}$, equations (12) and (13) can be given as:

$$^t[K_T]\ ^t\{\Delta U_e\} = ^{t+\Delta t}\{R_e\} - ^t\{F_e\} \tag{24}$$

Hence, in the static case the equilibrium throughout the deformation of the structure is accomplished exclusively between the external and the internal generalized forces. The equilibrium condition yields the incremental displacements (mechanical and electrical) between two successive configurations. The stiffness matrix is not constant (as it is assumed in the linear analysis) due to the continuously changing configuration. Therefore, the governing nonlinear equation is linearized through the tangential stiffness matrix, which also takes into account the stress field in the previous configuration. The discrete update of the tangential stiffness matrix is performed after each incremental time step. However, the tangential stiffness matrix undergoes a continuous change during the deformation. For that reason the modified Newton-Raphson method is used to improve the accuracy of the solution based on the linearized equations. In this method the tangential stiffness matrix is calculated at the beginning of the increment and then kept constant for all the iterations within that increment, thus avoiding the expense of recalculating and factorizing the tangential stiffness matrix in each iterative step.

5. DEGENERATED SHELL ELEMENT IN GEOMETRICALLY NONLINEAR FORMULATION

The degenerated shell element described in the first part of the paper [6] is a Mindlin type of element allowing transverse shear strains and stresses, it utilizes full biquadratic shape functions since it has 9 nodes, 6 degrees of freedom per node (3 displacements and 3 rotations) and it has additionally as many electric degrees of freedom (difference of electric potential) as there are piezoelectric layers across the thickness of the element. The element uses the equivalent-single layer based approach for modeling multilayered material with directionally dependent material properties (Fig. 2).
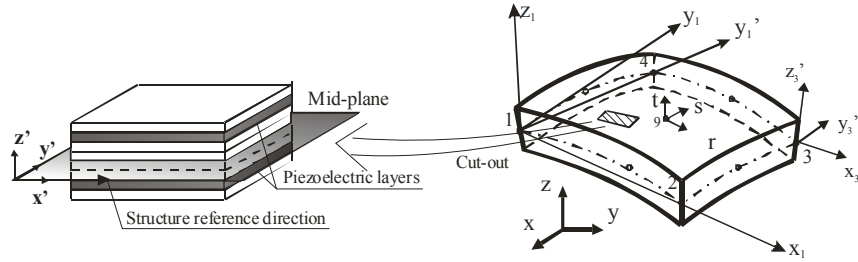

Fig. 2. Equivalent-single layer based approach for modeling multilayered material

Only the additional element matrices and vectors, which are used within the geometrically nonlinear formulation and are therefore not given in the first part of the paper, will be described here.

The geometrical stiffness matrix (initial stress matrix) due to the stress in the previous configuration is calculated in the following manner (see (19)):

$$[K]_\sigma = \int_V [G]^T [\sigma][G]dV \tag{25}$$

with matrix $[G]$ defined by (14) and $[\sigma]$ by (16). Within the partial derivatives of the displacements the terms related to displacements, $[G_T]$, can be distinguished from those related to the rotations, $[G_R]$. Furthermore, considering latter, the distinction can be made between the terms constant with respect to the thickness coordinate, $[G_{R0}]$, and the terms that are linear with respect to the thickness, $[G_{R1}]$. Taking advantage of the notations introduced in the first part of the paper [6], it can be written:

$$[G_{Ti}] = \begin{bmatrix} l_1 B'(1,i) & m_1 B'(1,i) & n_1 B'(1,i) \\ l_1 B'(2,i) & m_1 B'(2,i) & n_1 B'(2,i) \\ l_1 B'(3,i) & m_1 B'(3,i) & n_1 B'(3,i) \\ l_2 B'(1,i) & m_2 B'(1,i) & n_2 B'(1,i) \\ l_2 B'(2,i) & m_2 B'(2,i) & n_2 B'(2,i) \\ l_2 B'(3,i) & m_2 B'(3,i) & n_2 B'(3,i) \\ l_3 B'(1,i) & m_3 B'(1,i) & n_3 B'(1,i) \\ l_3 B'(2,i) & m_3 B'(2,i) & n_3 B'(2,i) \\ 0 & 0 & 0 \end{bmatrix} \tag{26}$$

furthermore:

$$[G_{R0i}] = \frac{h}{2} N_i B'' \begin{bmatrix} 0 & 0 & 0 \\ 0 & 0 & 0 \\ C_{x'}(1,i) & C_{y'}(1,i) & C_{z'}(1,i) \\ 0 & 0 & 0 \\ 0 & 0 & 0 \\ C_{x'}(2,i) & C_{y'}(2,i) & C_{z'}(2,i) \\ 0 & 0 & 0 \\ 0 & 0 & 0 \\ 0 & 0 & 0 \end{bmatrix} \tag{27}$$

and finally:

$$[G_{R1i}] = \frac{h}{2} \begin{bmatrix} B'(1,i)C_{x'}(1,i) & B'(1,i)C_{y'}(1,i) & B'(1,i)C_{z'}(1,i) \\ B'(2,i)C_{x'}(1,i) & B'(2,i)C_{y'}(1,i) & B'(1,i)C_{z'}(1,i) \\ B'(3,i)C_{x'}(1,i) & B'(3,i)C_{y'}(1,i) & B'(1,i)C_{z'}(1,i) \\ B'(1,i)C_{x'}(2,i) & B'(1,i)C_{y'}(2,i) & B'(1,i)C_{z'}(2,i) \\ B'(2,i)C_{x'}(2,i) & B'(2,i)C_{y'}(2,i) & B'(2,i)C_{z'}(2,i) \\ B'(3,i)C_{x'}(2,i) & B'(3,i)C_{y'}(2,i) & B'(3,i)C_{z'}(2,i) \\ B'(1,i)C_{x'}(3,i) & B'(1,i)C_{y'}(3,i) & B'(1,i)C_{z'}(3,i) \\ B'(2,i)C_{x'}(3,i) & B'(2,i)C_{y'}(3,i) & B'(2,i)C_{z'}(3,i) \\ 0 & 0 & 0 \end{bmatrix} \quad (28)$$

Now, a typical term of the geometrical stiffness matrix is given in the following form:

$$[K_{ij}]_\sigma = \int_{-1}^{+1}\int_{-1}^{+1}\int_{-1}^{+1} \begin{bmatrix} [G_{Ti}]^T \\ -\,-\,-\,-\,-\,-\,-\,-\,-\,- \\ [G_{R0i}]^T + t[G_{R1i}]^T \end{bmatrix} [\sigma]\,[[G_{Tj}]\,|\,[G_{R0i}]+t[G_{R1j}]]\det[J]drdsdt \quad (29)$$

Due to the kinematical assumptions of the first-order shear deformation theory and different stiffness of layers, the stress is not a continuous function with respect to the thickness coordinate. However, layer-wisely it is a continuous function. Furthermore, layer-wisely it is a linear function with respect to the thickness coordinate in the local-running c. s., which continuously rotates with the element. Hence, the analytical integration in the thickness direction has to be performed in a layer-wise manner, yielding:

$$[K_{ij}]_\sigma = \int_{-1}^{+1}\int_{-1}^{+1}\sum_{n=1}^{N_L} \begin{bmatrix} [G_{Ti}]^T\int_{t_{n-1}}^{t_n}[\sigma_n]dt[G_{Tj}] & | & [G_{Ti}]^T\int_{t_{n-1}}^{t_n}[\sigma_n]dt[G_{R0j}]+[G_{Ti}]^T\int_{t_{n-1}}^{t_n}t[\sigma_n]dt[G_{R1j}] \\ -\,-\,-\,-\,-\,-\,-\,-\,- & + & -\,-\,-\,-\,-\,-\,-\,-\,-\,-\,-\,-\,-\,-\,-\,-\,- \\ [G_{R0i}]^T\int_{t_{n-1}}^{t_n}[\sigma_n]dt[G_{Tj}]+ & | & [G_{R0i}]^T\int_{t_{n-1}}^{t_n}[\sigma_n]dt[G_{R0j}]+[G_{R0i}]^T\int_{t_{n-1}}^{t_n}t[\sigma_n]dt[G_{R1j}]+ \\ [G_{R1i}]^T\int_{t_{n-1}}^{t_n}t[\sigma_n]dt[G_{Tj}] & | & [G_{R1i}]^T\int_{t_{n-1}}^{t_n}[\sigma_n]dt[G_{R0j}]+[G_{R1i}]^T\int_{t_{n-1}}^{t_n}t^2[\sigma_n]dt[G_{R1j}] \end{bmatrix}\det[J]\,drds \quad (30)$$

where the summation runs over all N_L layers, and $[\sigma_n]$ is the function of the engineering stress matrix (contains a constant and a linear term) of the nth layer. The tangential stiffness matrix comprises the contribution of both the stiffness matrix used in the linear analysis and the geometric stiffness matrix, as defined by (19).

The internal forces are calculated according to (22). Making a distinction between the membrane-flexural (in-plane) stresses and the transverse shear stresses, and using once again the notation from the first part of the paper, it will be:

$$\{f_{int}\} = \int_V [B_L]^T \{\sigma\} \, dV = \int_V [[B_{mf}]^T \,\vert\, [B_s]^T] \begin{Bmatrix} \{\sigma_{mf}\} \\ -- \\ \{\sigma_s\} \end{Bmatrix} dV \,, \tag{31}$$

Representing the strain-displacement matrix in the developed form, the internal forces at node i are given as:

$$\{f_{int\,i}\} = \int_V \begin{bmatrix} [B_{Tmi}]^T & \vdots & [B_{Tsi}]^T \\ ----- & + & ----------- \\ t\,[B_{R1fi}]^T & \vdots & [B_{R0si}]^T + t[B_{R1si}]^T \end{bmatrix} \begin{Bmatrix} \{\sigma_{mf}\} \\ -- \\ \{\sigma_s\} \end{Bmatrix} dV . \tag{32}$$

As mentioned before, the stress field is not a continuous function with respect to the thickness due to different stiffness of the layers across the thickness and therefore the layer-wise analytical integration over the thickness is to be performed, yielding the internal forces at node i as:

$$\{f_{int\,i}\} = \int_{-1}^{+1}\int_{-1}^{+1} \sum_{n=1}^{N_t} \left\{ \begin{array}{c} [B_{Tmi}]^T \int_{t_{n-1}}^{t_n} \{\sigma_{mf_n}\} dt + [B_{Tsi}]^T \int_{t_{n-1}}^{t_n} \{\sigma_{s_n}\} dt \\ ---------------------------- \\ [B_{R1fi}]^T \int_{t_{n-1}}^{t_n} t\{\sigma_{mf_n}\} dt + [B_{R0si}]^T \int_{t_{n-1}}^{t_n} \{\sigma_{s_n}\} dt + [B_{R1si}]^T \int_{t_{n-1}}^{t_n} t\{\sigma_{s_n}\} dt \end{array} \right\} \det[J] dr ds \tag{33}$$

The derived matrices and vectors, together with those derived in the first part of the paper, allow the application of the 9-node degenerated shell element in the geometrically nonlinear analysis. A simple example demonstrates the behavior of the element.

6. NUMERICAL EXAMPLE

The following example is chosen in order to demonstrate the behavior of the element in the geometrically nonlinear analysis by applying the updated Lagrangian formulation of

Layer 1: Thickness 3 mm
Young's modulus E =2.1 10^5 N/mm^2
Poisson's ratio   v=0.3
Layer 2: Thickness 2 mm
Young's modulus E =1 10^4 N/mm^2
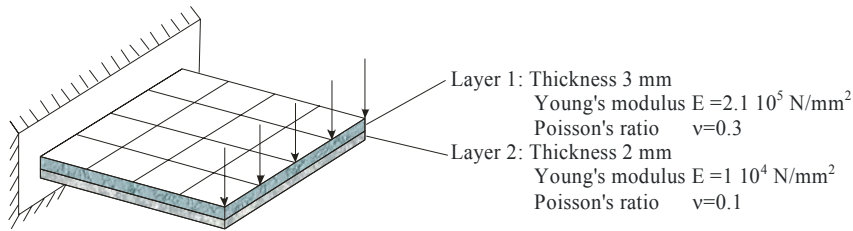Poisson's ratio   v=0.1

Fig. 3. Model of a clamped 2 layer plate with transverse forces acting on the free edge

the co-rotational approach. The authors have used the already existing solver and therefore the example covers only the pure mechanical field. The work on the extension of the

solver with the aim of solving coupled electro-mechanical field in the geometrically nonlinear analysis is in progress. A clamped plate with the in-plane dimensions 40×40 mm and the thickness of 5 mm is considered. The plate is made of composite material - two layers of different materials, the properties of which are given in Fig. 3. The plate is discretized by the 4x4 finite element mesh and the same vertical force of 3.3 kN acting downwards is applied at all nodes on the free edge of the plate.

The diagrams in Figs. 4 and 5 show the prediction of the transverse deflection and the longitudinal displacement of the plate mid-line with the assumptions of linearity and nonlinearity taken into account. The linear solution is obtained as one increment solution, while the given nonlinear solution is obtained throughout 400 increments. The accuracy of the solution is directly affected by the number of incremental steps. As was already emphasized, the higher the number of incremental steps, i.e. the smaller the incremental step, the better the accuracy of the result. Hence, the increase of the number of incremental steps results in the convergence of the obtained solution. In this specific case the convergence can be recognized for approximately 100 incremental steps, but the results are given for the last performed analysis with 400 incremental steps.

As expected in this case, the predicted transverse deflection based on the linear assumptions overestimates the actual, nonlinear result but, as can be seen in Fig. 4, the nonlinear effect is not strongly pronounced. On the other hand, the diagram in Fig. 5 demonstrates what effect the assumption of linearity might have on the obtained result. This figure shows a significant difference between the linear and the nonlinear prediction of the longitudinal displacement along the plate mid-line.
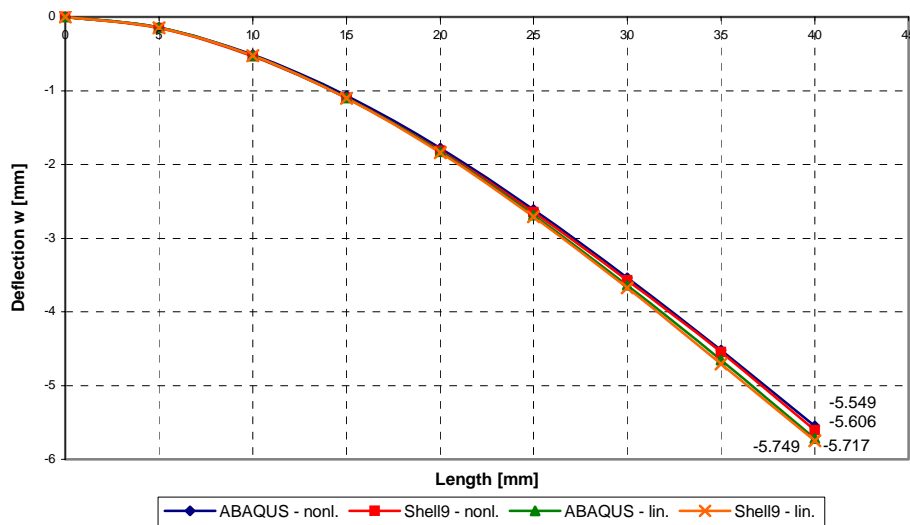

Fig. 4.   Comparison of linear and nonlinear prediction of transverse deflection (ABAQUS shell element and here developed shell9 element)
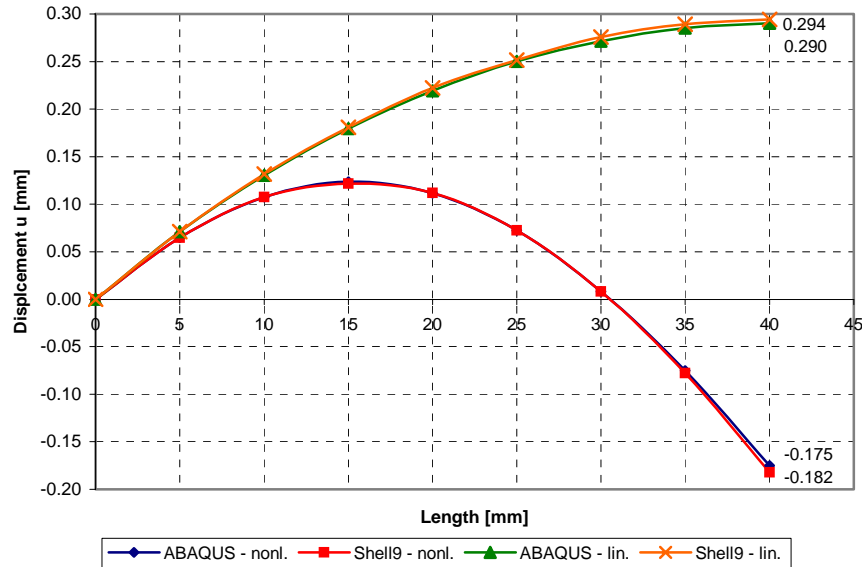
Fig. 5. Comparison of linear and nonlinear prediction of longitudinal displacement
(ABAQUS shell element and here developed shell9 element)

The free edge mid-point is chosen as a representative point and all the results from the diagrams in Figs. 4 and 5 are summarized in Table 1 for this point.

Table 1. Clamped plate case – comparative results from ABAQUS shell and shell9 element

Comparative results	Linear solution	Nonlinear solution
Free edge mid-point	Transverse deflection	
Abaqus shell element (8 nodes)	−5.717 mm	−5.549 mm
Shell9 (9 nodes)	−5.749 mm	−5.606 mm
Free edge mid-point	Longitudinal displacement	
Abaqus shell element (8 nodes)	+0.290 mm	−0.175 mm
Shell9 (9 nodes)	+0.295 mm	−0.182 mm

7. CONCLUSIONS

The paper points out the fact that results of an analysis can be significantly influenced by the assumptions made before the analysis is performed. The assumptions of the linear analysis require less numerical effort, but they have to be justified, otherwise the predicted behavior of the structure might suffer on accuracy. The choice between the linear and the nonlinear analysis lies on the engineering judgment. However, considering the active thin-walled structures, a need for a model that takes into account geometrically and/or materially nonlinear effects is demonstrated by a number of investigations.

The paper considers the active thin-walled structures made of piezoelectric composite laminates, which are susceptible to relatively large transverse deflections while exhibiting small strains. This case corresponds to the geometrically nonlinear formulation. The continuously changing configuration requires the introduction of either auxiliary strain and stress measures, or an auxiliary (co-rotational) coordinate system. The latter solution is adopted in the present formulation. The updated Lagrangian formulation of the problem is chosen because it facilitates the extension of the formulation into full nonlinear. This is especially important for the piezoelectric active structures due to the nonlinear behavior of the piezoelectric coupling even for small maximal values of the electric field [9]. It is intended in the future work of the authors to extend the present formulation with the aim of including this type of nonlinearity.

The first part of the paper, which pertains to the linear analysis, represents the 9-node degenerated shell element as a suitable numerical tool for the finite element analysis of the active structures that are dealt with here. Based on the considerations given at the beginning of the second part of the paper, the element is extended so that it can be used within the frame of the geometrically nonlinear analysis. The so-developed degenerated shell element is integrated in a special module of COSAR (www.femcos.de) originally developed for the nonlinear dynamic analysis of large scale systems. Nevertheless, it can also be used to perform the linear and nonlinear static analysis by means of the dynamic relaxation technique. The behavior of the element is demonstrated through a simple example of static analysis. The present work of the authors is focused on the extension of the solver so that geometrically nonlinear dynamic analyses can also be performed for the coupled electro-mechanical field.

REFERENCES

1. Bathe K. J.: "Finite element procedures in engineering analysis", Prentice-Hall, Inc., Englewood Cliffs, New Jersey, 1982.
2. Belytschko, T., Hseih, B. J.: "Non-linear transient finite element analysis with convected co-ordinates", Int. J. Num. Meth. Engng, Vol. 7, pp. 255-271, 1973.
3. Belytschko, T., Glaum, L. W.: "Applications of higher order corotational stretch theories to nonlinear finite element analysis", Computers & Structures, Vol. 10, pp. 175-182, 1979.
4. Criesfield, M. A.: "Non-linear finite element analysis of solids and structures, Volume1: Essentials", John Wiley & Sons, 1997.
5. Carrera, E.: "An improved Reissner-Mindlin-type model for the electromechanical analysis of multilayered plates including piezo-layers", Journal of intelligent material systems and structures, Vol. 8, pp. 232-248, 1997.
6. Marinković, D, Köppe, H., Gabbert, U.: "Finite element development for generally shaped piezoelectric active laminates, part I - linear approach", Facta Universitatis: Series of mechanical engineering, Vol. 2, Issue , 2004.
7. Mattiason, K., Bengtsson, A., Samuelssonn A.: "On the accuracy and efficiency of numerical algorithms for geometrically nonlinear structural analysis", in Bergan, P. G., Bathe, K. J., Wunderlich, W (Eds.): "Finite element methods for nonlinear problems", Springer-Verlag, 1985.
8. Mesecke-Rischmann, S.: "Modellierung von flachen piezoelektrischen Schalen mit zuverlässigen finiten Elementen", Dissertation, Helmut-Schmidt-Universität / Universität der Bundeswehr Hamburg, 2004.
9. Rosen C. Z. et al (eds).: Piezoelectricity, American Institute of physics, New York, 1992.
10. Simoes Moita, J. M., Mota Soares, C. M., Mota Soares, C. A.: "Geometrically non-linear analysis of composite structures with integrated piezoelectric sensors and actuators", Composite structures, Vol. 57, pp. 253-261, 2002.
11. Varels, D, Saravanos, D.: "Nonlinear coupled mechanics and initial buckling of composite plates with piezoelectric actuators and sensors", Journal of Smart Materials and Structures, Vol. 11, Issue 3, pp. 330-336, 2002.
12. Yi, S., Ling, S. F., Ying, M.: "Large deformations finite element analyses of composite structures integrated with piezoelectric sensors and actuators", Finite elements in analysis and design, Vol. 35, pp. 1-15, 2000.

RAZVOJ KONAČNOG ELEMENTA ZA KOSTRUKCIJE OPŠTEG OBLIKA OD KOMPOZITNIH LAMINATA SA PIEZOELEKTRIČNIM KOMPONENTAMA DEO II – GEOMETRIJSKI NELINEARNI PRISTUP

Dragan Marinković, Heinz Köppe, Ulrich Gabbert

Tankozide konstrukcije sa piezoelektričnim komponentama, posebno one sa primetno većom membranskom od savojne krutosti, su podložne velikim ugibima. Ispitivanja brojnih istraživača sprovedena poslednjih godina pokazuju da na veličinu ugiba, frekvenciju oscilovanja, izlazni električni napon i druge veličine od značaja osetno mogu uticati pretpostavke velikih pomeranja i deformacija konstrukcije. Iz tog razloga drugi deo rada proširuje formulaciju datu u prvom delu na geometrijski nelinearnu analizu, čineći pretpostavku malih deformacija ali velikih pomeranja. Iskorišćen je korotacioni pristup. Razvijene su linearizovane jednačine metode konačnih elemenata za geometrijski nelinearnu analizu piezoelektričnog kontinuuma i primenjene pomoću konačnog elementa tipa "degenerisane ljuske" sa 9 čvorova koji je već opisan u prvom delu rada.

Ključne reči: *geometrijski nelinearna analiza, aktivna konstrukcija, konačni element tipa ljuske, piezoelektrične komponente.*